Armenian Journal of Physics, 2019, vol. 12, issue 1, pp. 1-16

Sensing Possibilities of Yb^{3+} Doped $Y_3A_5O_{12}$, $LiNbO_3$ and $NaBi(WO_4)_2$ Crystals

H. G. Demirkhanyan[1], G. G. Demirkhanyan[1,2], E. P. Kokanyan[1,2]

[1]*Armenian State Pedagogical University, 17 Tigran Mets ave., 0001, Yerevan, Armenia*
[2]*Institute for Physical Research, NAS of Armenia, 0203, Ashtarak, Armenia*
E-mail: dehasmik@gmail.com

Received 05 December 2018

Abstract: The possibilities of Yb^{3+} doped $Y_3Al_5O_{12}$, $LiNbO_3$ and $NaBi(WO_4)_2$ crystals as materials for optical temperature sensor (OTS) based on fluorescence intensity ratio (FIR), absorption coefficient ratio (ACR) and relative zero-phonon line intensity (ZPLI) techniques are discussed. The operating temperature regions and average sensitivity for the considered OTSs are determined. It is shown, that the ZPLI technique is more effective for OTS at cryogenic temperatures, whereas FIR and ACR one – at high (above room) temperature range**.**

Keywords: Yb^{3+} doped crystals, optical temperature sensors, fluorescence intensity ratio, absorption coefficient ratio, zero-phonon line intensity.

1. Introduction

Recently, there are many researches for new optical sensors possibilities because of their high sensitivity and wide range of application areas (chemical and biochemical changes, measurement of deformations, temperature, pressure etc.). Optical temperature sensors (OTS) are a special case among optical sensors. These can be effectively used for measurement and control of temperature, in cases where conventional techniques cannot be used and/or have significant drawbacks (highly corrosive media, electrical power stations, oil refineries, coal mines and fire detection systems). They have significant advantages compared to conventional ones in remote sensing possibility, electrical passiveness, greater sensitivity, protection from electromagnetic noise, and wide acting range.

Rare earth (RE^{3+}) ions doped materials (particularly dielectric crystals) are well known from the point of view of the temperature dependences of spectroscopic characteristics (fluorescence intensities, fluorescence lifetimes, absorption coefficients etc.) in the infrared and visible range. This makes them good candidates for OTS. So far, OTSs on the base of different RE^{3+} ions ($Er^{3+}, Sm^{3+}, Eu^{3+}, \mathrm{Pr}^{3+}$) doped glasses, ceramics and fibers have been presented [1-4]. OTSs on above mentioned materials have ability to cover a wide temperature range (300^0 to $1623^0 K$) with reasonable measurement resolution [3-7]. However, not much research work has been carried out on Yb^{3+} doped materials for such purpose. Usually, Yb^{3+} is used as a sensibilizator to enhance efficiency of up-conversion luminescence of erbium, holmium, thulium ions, etc. [8-10]. J. L. Kenndey at al. [9]have reported the fiber-optic temperature sensors based on fluorescence decay in Yb^{3+} doped yttrium aluminum garnet (YAG) and YAG: Yb^{3+}, Tb^{3+}. S.A. Wade et al. [11] have reported the fluorescence intensity ratio (FIR) based temperature sensing performance of Yb^{3+} doped silica fiber using Stark sublevels of $^2F_{5/2}$ manifold of Yb^{3+} ion.

In this paper, we discuss sensing properties of Yb^{3+} doped $LiNbO_3(LN), Y_3Al_5O_{12}(YAG)$ and

$NaBi(WO_4)_2$ (NBW) crystals based on FIR, absorption coefficient ratio (ACR), as well as on zero-phonon line intensity (ZPLI) of fluorescence techniques.

2. Technology

There are several optical sensing techniques based on RE^{3+} ions doped materials. The operation of OST is based on the temperature dependences of the measurable spectroscopic and/or kinetic characteristics $R(T)$ of the optical spectra of an impurity ion, as such intensity or lifetime of fluorescence, absorption coefficient etc. The sensitivity of OTS based on measurement of a temperature dependent spectroscopic characteristic, $R(T)$, is defined by the relation

$$S_R(T) = \frac{1}{R}\frac{dR}{dT} \tag{1}$$

In general, the sensitivity defined by (1) itself depends on temperature and can have the quite complex analytical forms. Therefore, as a quantitative characteristic for OTS, it is convenient to use the average sensitivity defined by the expression

$$\overline{S}_R = \frac{1}{\Delta T}\int_{T_1}^{T_2} S(T)\,dT \tag{2}$$

where $\Delta T = T_2 - T_1$ is width of operational temperature range.

For searching new materials and mechanisms for temperature sensing it is necessary to consider, that thermal coupled operating energy levels of OTS must satisfy the following conditions:

1. Energy gap between initial levels
   - must be at least $\sim 200 cm^{-1}$ to guarantee the required solvability of corresponding spectral lines,
   - must not exceed $\sim 2000 cm^{-1}$ to ensure the required population of the initial levels in a given temperature range.
2. The energy gap between the initial level and the nearest lower level should be enough large (more than 6 times larger than Debye phonon energy of considered material) to guarantee domination of radiative transitions over non-radiative.

2.1 Fluorescence Intensity Ratio Technique

In fluorescence intensity ratio (FIR) technique as a temperature dependent value (R) the fluorescence intensities ratio is considered (Fig.1a):

$$R_{FIR} = \frac{I_{jo}}{I_{io}} = B\exp\left(-\frac{E_{ji}}{kT}\right) \tag{3}$$

where I_{jo} and I_{io} are intensities of spectral lines of corresponding transitions starting from thermally coupled levels i and j (Fig. 1a), ΔE_{ji} is energy gap between initial levels, k is Boltzmann's coefficient, T is temperature, B is temperature independent value [1,2]

$$B = \frac{g_j \sigma_{jo} \nu_{jo}}{g_i \sigma_{io} \nu_{io}}, \tag{4}$$

where $\sigma_{\mu o}$ and $\nu_{\mu o}$ are cross-section and frequency of $\mu \to 0$ transition, g_μ is degeneracy of level μ. It is assuming, that temperature dependence, R_{FIR}, is conditioned by Boltzmann factor of population of neighboring energy levels [1-7]. It is assumed, that the speed of thermalization between two excited i and j levels is larger compared to the probability of spontaneous transitions from i and j levels: A_{io} and A_{jo}. For Yb^{3+} doped crystal, in which we should consider inter-Stark transitions, the expression (4) can be transformed as follow. At first, we use the expression for peak value of cross-section

$$\sigma_{\mu o} = \frac{\lambda_{\mu o}^2}{16\pi^2 \Gamma_{\mu o}} A_{\mu o}$$

and, second, we consider that $A_{jo} \sim \nu_{jo}^3 n_{jo} S_{jo}$. Then the expression (3) is transformed to the form

$$B = \frac{g_j n_{io}^3 \lambda_{io}^2 \Gamma_{io} S_{jo}}{g_i n_{jo}^3 \lambda_{jo}^2 \Gamma_{jo} S_{io}} \tag{5}$$

Here n is refractive index at the transition wavelength λ, Γ is linewidth and S is line strength of corresponding transition.

Note, that, in this case, the dependence of R_{FIR} on temperature is determined by both Boltzmann factor and homogeneous widths of the corresponding spectral lines. However, compared to Boltzmann factor the temperature dependence of the ratio $\Gamma_{i\mu_p} / \Gamma_{j\mu_k}$ is weak, and, as a rule, it can be neglected. Thus, sensitivity of OST based on FIR technique is defined via a simple expression

$$S_R(T) = \frac{\Delta E_{ji}}{kT^2} \tag{6}$$

and average sensitivity at the $[T_1, T_2]$ temperature range –

$$\overline{S}_{FIR} = \frac{\Delta E_{ji}}{kT_1 T_2} \tag{7}$$

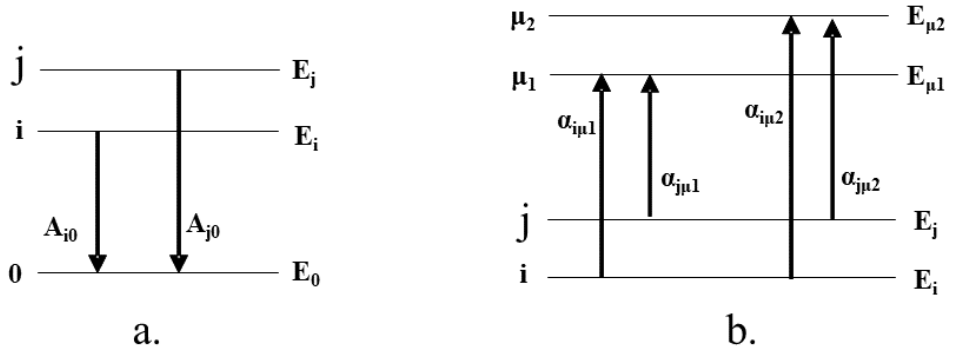

Fig. 1. OTS's schemes operated on (a) FIR and (b) ACR techniques.

2.2 Absorption Coefficients Ratio Technique

The scheme of absorption coefficients ratio (ACR) technique is given in Fig.1(b). The absorption coefficients ratio from two thermally coupled levels i and j is used as a temperature-dependent measure value (R). Wherein, the final state of transitions may be either one level or two different levels, depending on line strengths of corresponding transitions.

For Yb^{3+} doped crystal, by taking into account that the energy levels shift during electron transitions is less than width of corresponding spectral line, the absorption coefficients ratio from ground and first excited states (transitions $i \to \mu_p$ and $j \to \mu_k$)may be presented by the next expression given in [12]

$$R_{ACR} = \frac{\alpha_{j\mu_k}}{\alpha_{i\mu_p}} = D\exp\left(-\frac{\Delta E_{ji}}{kT}\right), \tag{8}$$

where D is determined by the expression

$$D = \frac{n_{i\mu_p}^2 \lambda_{i\mu_p} \Gamma_{i\mu_p} S_{j\mu_k}}{n_{j\mu_k}^2 \lambda_{j\mu_k} \Gamma_{j\mu_k} S_{i\mu_p}}, \tag{9}$$

Note, that like the FIR techniqueit is often assumed, that temperature dependence $R_{ACR}(T)$ is determined by Boltzmann factor of neighboring energy levels' population, and thermal coupled operating energy levels of OTS satisfy the above-mentioned conditions. Then the sensitivity $S_{ACR}(T)$ and the average sensitivity $\overline{S}_{ACR}$ will be determined by similar to (6) and (7) expressions.

2.3 Zero-Phonon Line Intensity Technique

Zero-phonon line intensity (ZPLI) techniques based on temperature dependence of intensity of zero-phonon line induced by inter-Stark transitions. As a temperature-dependent value, the relative intensity of the most intense zero-phonon spectral line is considered [12]

$$R_{ZPLI} = \frac{I(T)}{I(T_0)} = B \times \frac{\Gamma(T)}{\left[\Delta\varepsilon(T)\right]^2 + \Gamma^2(T)} \exp\left[-2M(T)\right] \tag{10}$$

where $\Gamma(T), \Delta\varepsilon(T)$ and $2M(T)$ are homogenous width, shift and Debye-Waller (D-W) factor of zero-phonon spectral line, respectively, $B = \left\{\left[\Delta\varepsilon(T_0)\right]^2 + \Gamma^2(T_0)\right\}\Gamma^{-1}(T_0)\exp\left[2M(T_0)\right]$ is determined at fixed T_0 temperature.In general, the sensitivity of ZPLI techniqueis defined by

$$S_{ZPLI} = 2\frac{dM}{dT} + \frac{1}{\Gamma}\frac{d\Gamma}{dT} + \frac{2(\Delta\varepsilon)^2}{(\Delta\varepsilon)^2 + \Gamma^2} \times \left[\frac{1}{\Delta\varepsilon}\frac{d\Delta\varepsilon}{dT} - \frac{1}{\Gamma}\frac{d\Gamma}{dT}\right]. \tag{11}$$

Or assuming that $\Delta\varepsilon \approx 0$ and neglecting third term in (11), we obtain

$$S_{ZPLI} = 2\frac{dM(T)}{dT} + \frac{d\ln\Gamma(T)}{dT}. \tag{12}$$

Then, the average sensitivity in temperature range $T_1 \le T \le T_2$ is defined by

$$\overline{S}_{ZPLI} = 2\Delta M + \ln\frac{\Gamma(T_2)}{\Gamma(T_1)}, \tag{13}$$

where $\Delta M = M(T_2) - M(T_1)$.

3. Yb^{3+} doped crystals: sensing possibilities on the base of FIR, ACR and ZPLI techniques

As known the energy scheme of the Yb^{3+} ion ($4f^{13}$ electronic configuration) consists of $^2F_{7/2}$ and $^2F_{5/2}$ manifolds, which are split into Stark sublevels in a crystalline field (Fig.2). Thereby, for studying spectroscopic properties of Yb^{3+} doped crystals, Stark structure of the optical spectrum of the impurity ion should be considered. All above mentioned sensing techniques applied to the Yb^{3+} doped YAG, LN and NBW crystals are presented below. The principle possibility of the use of Yb^{3+} doped YAG, NBW and LN crystals as materials for OTS have reported in [12-14].

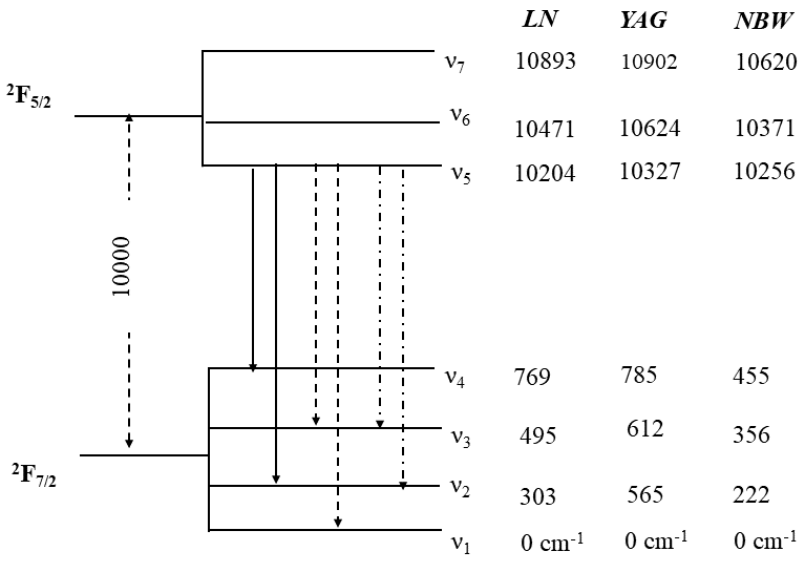

Fig. 2. Energy levels schemes of Yb^{3+} ion and transitions in LN (solid), YAG (dash) and NBW (dash-dot) crystals.

3.1. YAG-Yb^{3+}crystal

The main spectroscopic and kinetic characteristics of YAG: Yb^{3+} crystal (the line strengths and cross - sections of inter-Stark transitions, absorption coefficients, etc.) are determined in [15-17]. The results of experimental and theoretical investigations of temperature dependences of ZPLI at $960-1030\,nm$ range are given in [18, 19]. The values of the main spectroscopic characteristics required for subsequent quantitative estimates of sensing characteristics of YAG: Yb^{3+} crystal are given in Table 1.

Table 1. Spectroscopic characteristics of YAG: Yb^{3+} crystals.

Transition	$\nu_1 \to \nu_5$	$\nu_2 \to \nu_7$	$\nu_2 \to \nu_6$	$\nu_5 \to \nu_3$	**Ref.**
Wavelength, nm	968.3	967.4	994.1	1029.3	[15]
Line strength, 10^{-20}cm^2	0.1016	0.0717	0.1711	0.1878	[17]
Width of ZPL, cm^{-1} $500-1000^oK$ $77-300^oK$	 10.7 - 27.2 0.1-4.6	 54.0-95.8 25.6-38.2	 43.9- 87.2 14.9-27.6	 16.3-39.8 0.2-7.2	[19]
D – W's factor $500-1000^oK$ $77-300^oK$	 0.03-0.06 0.01-0.02	 0.44-0.84 0.17-0.29	 2.12-4.05 0.80-1.39	 13.68 - 26.19 5.17-9.0	[19]

3.1.1. YAG: Yb^{3+} sensors based on the ZPLI technique

The sensing property of YAG:Yb^{3+} crystal based on ZPLI technique is reported in [12]. As

shown in [18, 19] the intensity of fluorescence at $1029.3nm$ wavelength increases sharply when temperature drops below nitrogen values. Therefor the YAG: Yb^{3+} crystal is perspective material for ZPLI-based OTSs in the cryogenic temperature range: temperature dependences of relative intensity $I(T)/I(T_0)$ $\left(T_0 = 77^oK\right)$ spectral line at $1029.3nm$ and corresponding sensitivity determined by (12) are given in Fig.3. It is seen that when the temperature is decreased from 100^oK
to 10^oK, the radiation intensity increases by factor of 12. That provides high sensor sensitivity on the ZPLI technique (the average sensitivity is $3.4\%\times K^{-1}$). At the same time, in the temperature range $30-77^0K$, the dependence of the intensity ratio on temperature is nearly linear. The main characteristics of the OTS based on ZPLI technique are given in Table 1.

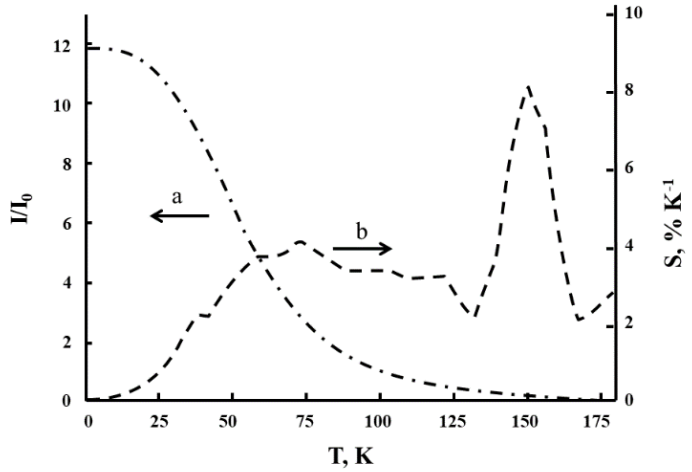

Fig. 3. Temperature dependence of (a) relative intensity of fluorescence on 1029.3nm wavelength and (b) OTS's sensitivity of ZPLI method for YAG:Yb^{3+} crystal.

3.1.2. YAG: Yb^{3+} sensors on the ACR technique

The sensing property of YAG: Yb^{3+} crystal based on ACR technique is investigated in [12]. From the energy levels scheme of the Yb^{3+} ion in YAG it is seen that the first excited Stark level ν_2 is separated from ground level ν_1 by energy gap of $565cm^{-1}$(Fig. 2). Thus, ACR technique can be effective at sufficiently high temperatures $\left(T \geq 500^oK\right)$, providing the necessary population $(\sim 20\%)$ of ν_2 excited level.Temperature dependences of the absorption coefficient ratio $R_{ACR}(T)$ at wavelengths of 994.1nm and 968.3nm and the sensitivity $S(T)$ are given in Fig. 4.It is seen that in temperature range $500-1000^oK$ the absorption coefficient ratio smoothly, almost linearly changes by the factor of two, which makes it possible to register temperature with 50^oK step at an average sensitivity of $\overline{S}_{ACR} = 0.16\%\times K^{-1}$.

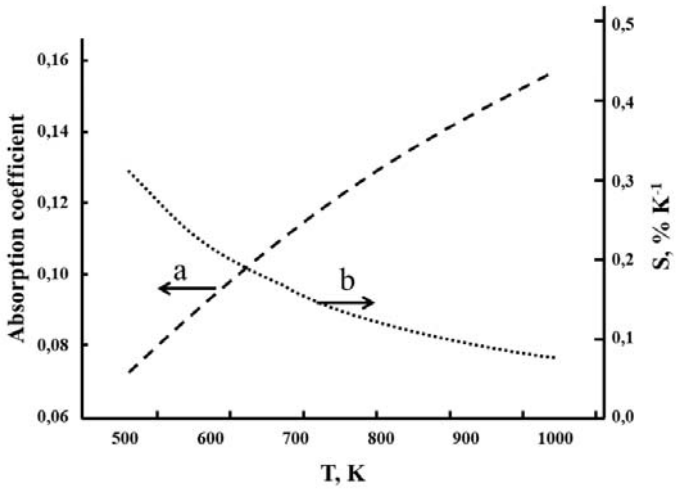

Fig.4. Temperature dependence of (a) absorption coefficient ratio on 994.1 and 968.3 nm wavelength; (b) OTS's sensitivity of ACR technique for YAG: Yb^{3+} crystal.

3.1.3. YAG:Yb^{3+} sensors on the FIR technique

As a temperature – dependent value we considered the ratio of the two most intensive emission lines starting from ground and first excited Stark sublevels of $^2F_{5/2}$ manifold correspond to two transitions $\nu_5 \to \nu_3$ $\left(\lambda_{\nu_5,\nu_3} = 1029.3\,nm\right)$ and $\nu_6 \to \nu_2$ $\left(\lambda_{\nu_6,\nu_2} = 994.1\,nm\right)$. By using the temperature dependences of the line widths Γ_{ν_5,ν_3} and Γ_{ν_6,ν_2} given in [19] and the values of line strengths $S_{\nu_5,\nu_3} = 0.188\times10^{-20}\,cm^2$ and $S_{\nu_6,\nu_2} = 0.171\times10^{-20}\,cm^2$ [17] we determined the temperature dependences $R_{FIR}(T)$ and the sensitivity $S_{FIR}(T)$ for considered wavelengths (Fig.5). It is seen, that optimal temperature region of operating is $300-1000K$ and then the average sensitivity according to (7) is $\overline{S}_{FIR} = 0.2\%\times K^{-1}$.

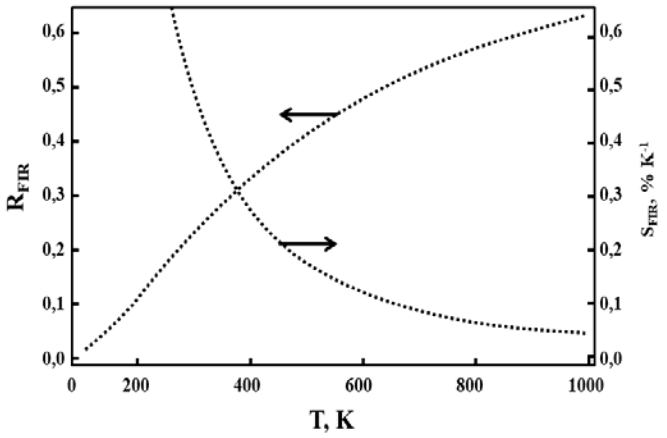

Fig.5. Temperature dependences of fluorescence intensities ratio on 1029.3 nm and 994.1 nm, and OTS's sensitivity of FIR method for YAG: Yb^{3+} crystal

3.2. LN- Yb^{3+} crystals

As seen in Fig. 2, the first excited Stark sublevels of both $^2F_{5/2}$ and $^2F_{7/2}$ manifolds are separated from the ground sublevels of corresponding manifolds by 303 and 267 cm^{-1} energy gaps. Thus, a disposition of energy sublevels of Yb^{3+} ion satisfies the above-mentioned conditions and LN:Yb^{3+} crystals may be considered as a potential material for OTS based on FIR and ACR techniques. The spectroscopic characteristics of LN:Yb^{3+} crystals are investigated in [20, 21].

The values of the main spectroscopic characteristics required for subsequent quantitative estimates of sensing characteristics of LN: Yb^{3+} crystal are given in Table 2. [20].

Table 2. Spectroscopic characteristics of LN: Yb^{3+} crystals.

Transition	$\nu_6 \to \nu_1$	$\nu_5 \to \nu_2$	$\nu_5 \to \nu_4$	**Ref.**
Wavelength, nm	**955**	**1010**	**1060**	
Line strength, $10^{-20}cm^2$	**0.8514**	**1.2287**	**0.8286**	**[20]**
Width of ZPL, cm^{-1}				
$100-600^oK$	**9.1–28.4**	**11.0-33.8**	**4.2 –18.0**	**[20]**
$150-350^oK$	**10.1–7.4**	**12.2–20.9**	**5.0–10.2**	
D – W's factor				
$100-600^oK$,	**3.83–.41**	**4.42–0.48**	**8.91–0.96**	**[21]**
$150-350^oK$	**2.08–.73**	**2.40–0.85**	**4.83–1.70**	

3.2.1. LN: Yb^{3+} sensors on the FIR technique

In the luminescence spectrum, a line at the 955*nm* wavelength is the only distinctly pronounced peak corresponding to the transition from the Stark sublevel ν_6 [20]. As it is seen in Fig.2, this peak corresponds only to the $\nu_6 \to \nu_1$ transition. On the other hand, in the luminescence spectrum, among the four lines, a peak with the maximum at 1060*nm*, correspond to the transition $\nu_5 \to \nu_4$. Therefore, as a temperature-dependent value the ratio of mentioned lines intensities, $R_{FIR} = I_{6\to1}/I_{5\to4}$ is considered [14].

The temperature dependences of $R_{FIR}(T)$ as well of sensitivity $S_{FIR}(T)$ were determined according to (3) - (5) by using the values in Table 2 and the temperature dependences of linewidths Γ_{61} and Γ_{54} given in Fig. 6 [21]. As seen, the temperature range $100-600K$ the dependences $R_{FIR}(T)$ with good accuracy is approximated by linear function, by which determines the operating range of OTS on FIR technique. In the temperature range under consideration the sensitivity changes from 3.95 to $0.12\%K^{-1}$. In particular, at room temperature it is $0.49\%\times K^{-1}$ [14]. The average value of sensitivity on this temperature range is $S_{av} = 0.704\%\times K^{-1}$.

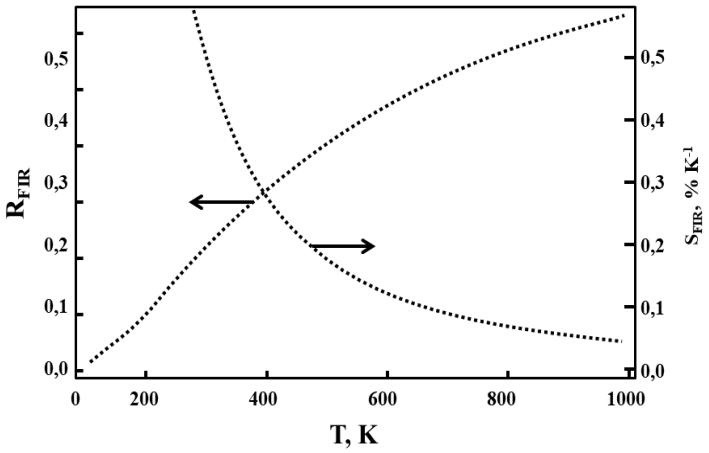

Fig.6. Temperature dependences $R(T)$ and $S(T)$ for FIR technique in LN-Yb^{3+}

3.2.2. LN: Yb^{3+} sensors on the ACR technique

As seen in Fig. 2, spectral lines at the wavelengths $1010nm$ ($\nu_2 \to \nu_5$ transition) and $955nm$ ($\nu_1 \to \nu_6$ transition) are most suitable to operate OST based on ACR technique. As a temperature-dependent measurable value the ratio of peak values of the absorption coefficients $R_{abs} = \alpha_{2\to5}/\alpha_{1\to6}$ at the mentioned wavelengths are considered. The temperature dependences of absorption coefficient ratio $R_{ACR}(T)$ and sensitivity $S_{ACR}(T)$, which were determined according to (8) and (9) by using the values in Table2 and the temperature dependences of linewidths $\Gamma_{16}(T)$ and $\Gamma_{25}(T)$ [21], are given in Fig.7. As seen in Fig. 7, in the temperature range $150-600K$ the dependence $R_{ACR}(T)$ with good accuracy is approximated by linear function, by which determines the operating range of OTS on ACR technique. In considered temperature range the average sensitivity is $S_{av} = 0.48\%K^{-1}$.

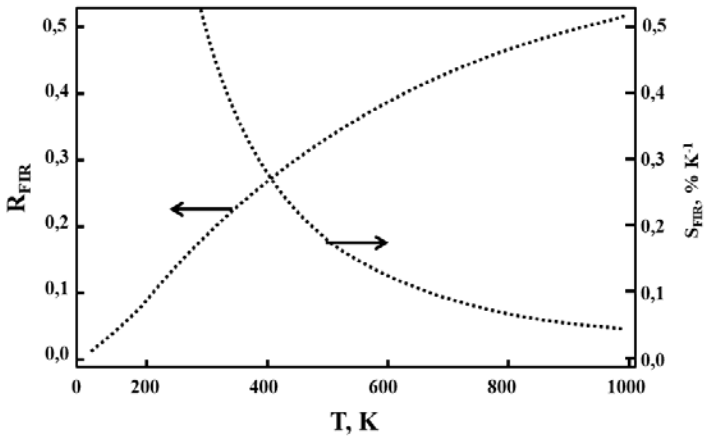

Fig. 7. Temperature dependences of $R(T)$ and sensitivity $S(T)$ for ACR methods in LN-Yb.

3.2.3. LN:Yb^{3+} sensors on the ZPLI technique

There are two intensive zero-phonon lines at 1010*nm* and 1060*nm* wavelengths in emission spectra of LN: Yb^{3+} . Therefore, as a temperature-dependent value for sensing on ZPLI techniques the intensities of impurity fluorescence at 1010*nm* and 1060*nm* wavelengths are considered. Temperature dependences of the relative intensities $I(T)/I(T_0)$ of fluorescence at considered wavelengths and of corresponding sensitivities are given in Fig. 8 [13]. As seen in Fig. 8, operating temperature range is $150^0 - 350^0 K$, for which the average sensitivities are $S_{av} = 0.97\% \times K^{-1}$ and $S_{av} = 0.66\% \times K^{-1}$ for the luminescence at 1010*nm* and 1060*nm* wavelengths respectively.

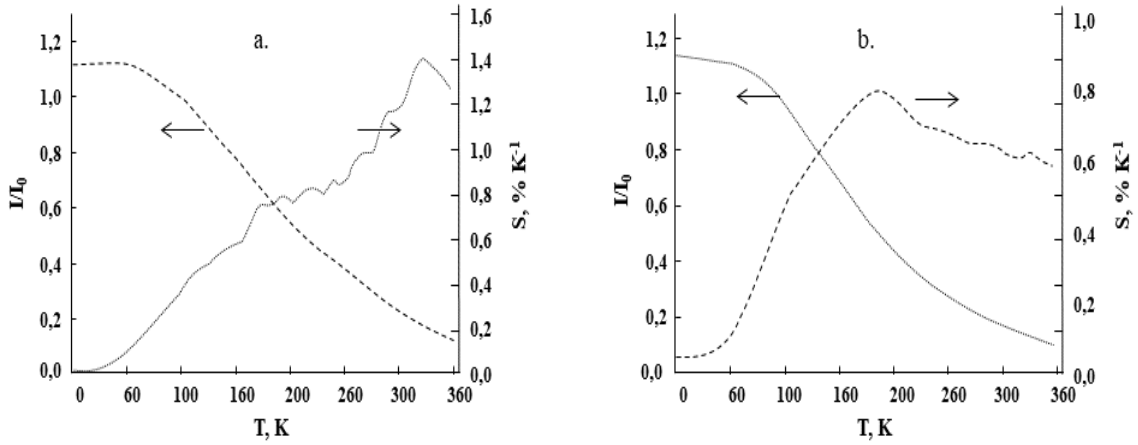

Fig.8. Temperature dependences of relative intensities and sensitivities of OTS based ZPLI techniques in LN: Yb^{3+} for luminescence at: a) 1010*nm* and b) 1060*nm* wavelength.

3.3. NBW: Yb^{3+} crystal

Spectroscopic characteristics of NBW: Yb^{3+} crystals due to the inter-Stark transitions are determined in [22, 23]. Temperature-dependent line widths and associated Debye–Waller factors (DWFs) for zero-phonon transitions between the Stark sublevels of the ${}^2F_J$ $(J = 7/2, 5/2)$ manifolds of Yb^{3+} in NBW are investigated, as well as the temperature dependences of the linewidths, DWFs and the intensities of the inter-Stark transitions are determined in [24].

Table 3. Spectroscopic characteristics of NBW: Yb^{3+} crystals.

Transition	$\nu_5 \to \nu_2$	$\nu_5 \to \nu_$	$\nu_6 \to \nu_1$	$\nu_6 \to \nu_2$	$\nu_6 \to \nu_3$	$\nu_7 \to \nu_2$	$\nu_7 \to \nu_4$	**Ref**
Wavelength, nm	**997**	**1010**	**964**	**985**	**998**	**962**	**984**	**[22]**
Line strength, 10^{-20}cm^2	**1.1560**	**0.90**	**1.0890**	**1.3912**	**0.5232**	**0.0643**	**1.0977**	**[24,25]**
Width of ZPL, cm^{-1}								
$300-1000^oK$	**17.3–48.1**	**6.8–24.4**	**13.0–56.5**	**23.0–70.4**	**12.5–46.7**	**27.3–66.6**	**16.0–38.7**	
$30-400^oK$	**8.9–21.6**	**1.0–9.3**	**1.9–18.9**	**10.8–29.6**	**2.9–17.2**	**17.6–32.7**	**10.2–19.1**	**[24,25]**
$50-150^oK$	**9.0–11.4**	**1.2–3.1**	**2.0–4.9**	**10.9–14.2**	**2.1–5.9**	**17.7–32.6**	**10.2–11.8**	
D – W's factor							$\times 10^{-3}$	
$300-1000^oK$	**5.4–1.5**	**1.1–0.3**	**1.6–0.5**	**0.8–0.2**	**6.3–1.8**	**16.3–4.6**	**3–0.9**	
$30-400^oK$,	**217–4.0**	**45.4–0.8**	**67.7–1.2**	**33.3–0.6**	**250–4.6**	**651–11.9**	**130–2.4**	**[24,25]**
$50-150^oK$	**81.5–13**	**17.0–2.7**	**25.4–4.0**	**12.5–2.0**	**93.8–15.0**	**246–38.9**	**48.7–7.8**	

3.3.1. NBW:Yb^{3+} sensors on the FIR technique

From NBW: Yb^{3+} crystal's luminescence spectrum it is seen that there are two intensive lines on $\sim 985nm$ and $\sim 997nm$. On the other hand, the analyses of the Stark structure of energy scheme shows, that there are two couples of inter-Stark transitions on these wavelengths, which are agreed with above mentioned conditions for FIR sensing technique. First couple is $\nu_6 \to \nu_2 \left(\lambda_{\nu_6,\nu_2} = 985.3nm\right)$, $\nu_7 \to \nu_4 \left(\lambda_{\nu_7,\nu_4} = 983.8nm\right)$ and the second is $\nu_5 \to \nu_2 \left(\lambda_{\nu_5,\nu_2} = 996.6nm\right)$, $\nu_6 \to \nu_3 \left(\lambda_{\nu_6,\nu_3} = 998.6nm\right)$.Therefore, in this case, the temperature - dependent parameter is defined by following expression

$$R_{FIR} = \frac{I_{62}+I_{74}}{I_{52}+I_{63}} = \left[\frac{S_{62}}{\lambda_{62}^2\Gamma_{62}}\exp\left(-\frac{\varepsilon_{65}}{kT}\right)+\frac{S_{74}}{\lambda_{74}^2\Gamma_{74}}\exp\left(-\frac{\varepsilon_{75}}{kT}\right)\right]\times\left[\frac{S_{52}}{\lambda_{52}^2\Gamma_{52}}+\frac{S_{63}}{\lambda_{63}^2\Gamma_{63}}\exp\left(-\frac{\varepsilon_{65}}{kT}\right)\right]^{-1} \quad (14)$$

Using the numerical values of the line strengths: $S_{62} = 1.39\times10^{-20}$, $S_{63} = 5.48\times10^{-20}$,

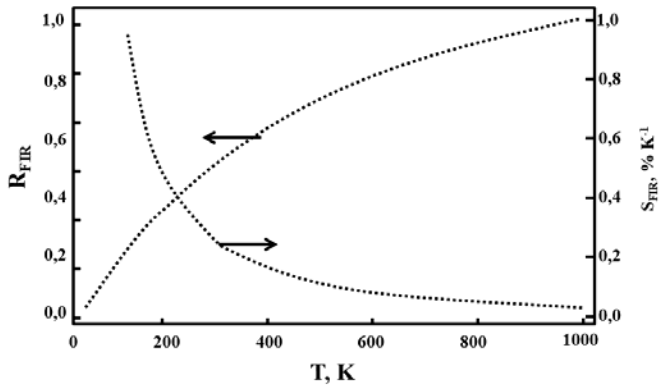

Fig. 9. Temperature dependences of fluorescence intensities ratio and OTS's sensitivity of FIR method for NAB: Yb3+ crystal.

$S_{74}=1.1\times10^{-20}$, $S_{52}=1.16\times10^{-20}$ (in cm^2) [23], as well the temperature dependencies of line widths: $\Gamma_{62}(T),\Gamma_{74}(T),\Gamma_{52}(T),\Gamma_{63}(T)$ given in [24], we determine the temperature dependences of R_{FIR} and of sensitivity S_{FIR} (Fig. 8). As seen in Fig. 9, the operating temperature range is, $\left[300^oK,1000^oK\right]$ and the average sensitivity is $S_{av}=0.095\%\times K^{-1}$.

3.3.2. NBW:Yb^{3+} sensors on the ACR technique

For determination of possibilities of ACR sensing technique in NBW:Yb^{3+} crystal, we analyzing absorption spectrum of this crystal, from which it is seen, that again we should consider, that there are two lines overlapping of two couples of inter-stark transitions: first couple is $\nu_2\rightarrow\nu_5\left(\lambda_{\nu_2\nu_5}=961.8nm\right)$, $\nu_3\rightarrow\nu_6\left(\lambda_{\nu_3\nu_6}=998.6nm\right)$ and the second is $\nu_1\rightarrow\nu_{\nu_6}\left(\lambda_{\nu_1\nu_6}=964.2nm\right)$, $\nu_2\rightarrow\nu_7\left(\lambda_{\nu_2\nu_7}=961.8nm\right)$. So, as a temperature dependent value

$$R_{ACR}=\frac{\alpha_{25}+\alpha_{36}}{\alpha_{16}+\alpha_{27}}=\left[\frac{\lambda_{25}S_{25}}{\Gamma_{25}}\exp\left(-\frac{\varepsilon_{21}}{kT}\right)+\frac{\lambda_{36}S_{36}}{\Gamma_{36}}\exp\left(-\frac{\varepsilon_{31}}{kT}\right)\right]\times\left[\frac{\lambda_{16}S_{16}}{\Gamma_{16}}+\frac{\lambda_{27}S_{27}}{\Gamma_{27}}\exp\left(-\frac{\varepsilon_{21}}{kT}\right)\right]^{-1}. \quad (15)$$

Using the numerical values of the line strengths: $S_{25}=1.16\times10^{-20}$, $S_{27}=6.43\times10^{-20}$, $S_{16}=1.09\times10^{-20}$, $S_{36}=5.23\times10^{-20}$ (in cm^2) [23] and the temperature dependencies of line widths: $\Gamma_{25}(T),\Gamma_{27}(T),\Gamma_{16}(T),\Gamma_{36}(T)$ [24], it was determined the temperature dependences of R_{ACR} and of sensitivity S_{ACR} (Fig.10). As seen in Fig.10, the operating temperature range is $\left[300^oK,1000^oK\right]$, for which the average sensitivity is $0.172\%\times K^{-1}$.

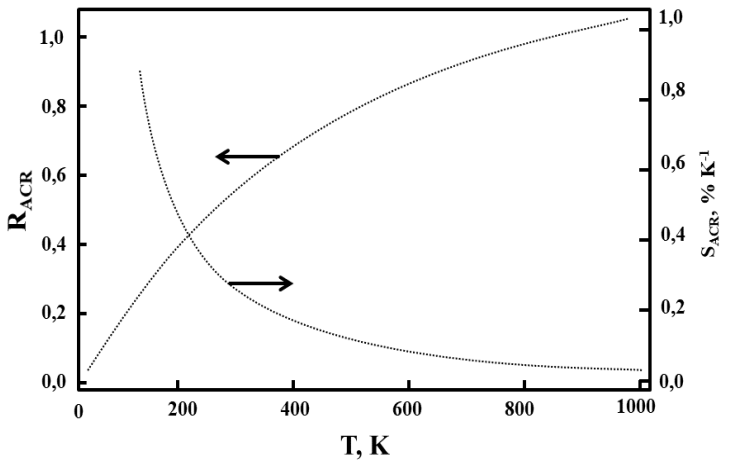

Fig. 10 Temperature dependence of (a) absorption coefficient ratio; (b) OTS's sensitivity of ACR method for NBW: Yb^{3+} crystal.

3.3.3. NBW:Yb^{3+} sensors on the ZPLI technique

There are two intensive zero-phonon lines at 1010*nm* and 996.6*nm* wavelengths in emission spectra of NBW: Yb^{3+} crystal corresponding to the inter-Stark transition $\nu_5 \to \nu_3$ and $\nu_5 \to \nu_2$. Therefore, as a temperature-dependent value for sensing on the ZPLI technique the intensities of fluorescence at these wavelengths are considered. Temperatures dependences of the relative intensities $R_{ZPLI} = I(T)/I(T_0)$ of fluorescent considered wavelengths and of corresponding sensitivities, which were determined by formulae (10) and (11), are given in Fig.11 [13]. As seen in Fig.11, operating temperature ranges are $[30^oK, 350^oK]$ and $[50^oK, 400^oK]$ for luminescence at 996.6*nm* and 1010*nm* wavelengths, respectively. Corresponding values of average sensitivities are 1.16 and $0.84\%K^{-1}$ for 1010 and 996.6*nm* wavelengths.

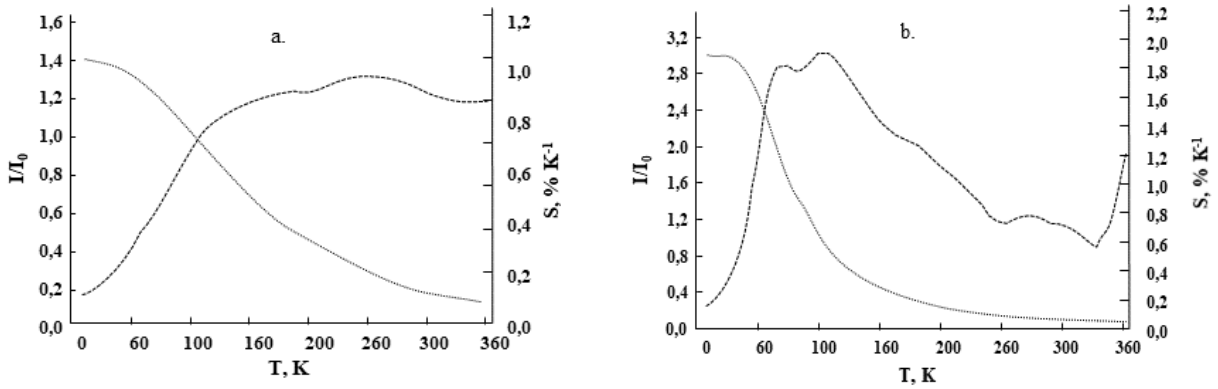

Fig.11. Temperature dependences of relative intensities and sensitivities of OTS based on NBW:Yb^{3+}:
a) 996.6 nm, b) 1010 nm.

4. Conclusion

Thus, the Yb^{3+} doped YAG, LN and NBW crystals can be considered as good materials for the OTSs based on FIR, ACR and ZPLI techniques and they can be used in the development of optical temperature sensors at wide temperature regions. In the temperature range of $(40-130K)$ for YAG: Yb^{3+}, $(50-300K)$ for LN: Yb^{3+} and $(50-300K)$ for NBW: Yb^{3+} crystals the temperature dependences of the ZPLI intensity with high accuracy $(\sim 0.1\%)$ approximates by a linear function, which increase the attractiveness of these materials as OTS. This mainly concerns to the YAG: Yb^{3+} crystal, the radiation intensity temperature sensitivity of which at the wavelength of 1030*nm* is "drastically" high. As a result the expected average sensitivity of the temperature sensor in the temperature range of $40-130K$ reaches a value of

$3.4\%\times K^{-1}$, which in the considered temperature range on one order of magnitude exceeds the average sensitivity of cooper-constantan thermocouples $(0.31\%\times K^{-1})$ and is nearly the same as for the chromel-constantan $(2.8\%\times K^{-1})$ one [1].On the other hand, the LN: Yb^{3+}, NBW: Yb^{3+} and YAG: Yb^{3+} based OTSs on the FIR and ACR technics effectively operate in high temperature range and its sensitivity is comparable to the sensitivity of other sensors (Table 4).

Table 4. Sensing characteristics of YAG: Yb^{3+}, LN: Yb^{3+} and NBW: Yb^{3+} crystals.

materials	technique	Maximal sensitivity $S_{max}(T_0)$, $\%\times K^{-1}$	Average sensitivity S_{av}, $\%\times K^{-1}$	Operating temperature range ΔT, K	Ref.
YAG: Yb^{3+}	FIR: $\nu_6 \to \nu_2 : \nu_5 \to \nu_3$	300K, 0.72	0.20	300-1000	-
	ACR: $\nu_2 \to \nu_6 : \nu_1 \to \nu_5$	500K, 0.31	0.16	500-1000	[12]
	ZPLI: $\nu_5 \to \nu_3$	75K, 4.21	3.40	40-130	[12]
	ZPLI: $\nu_5 \to \nu_1$	120K, 0.04	0.02	100-240	[12]
LN: Yb^{3+}	FIR: $\nu_6 \to \nu_1 : \nu_5 \to \nu_4$	100K, 1.96	0.71	100-600	[14]
	ACR: $\nu_2 \to \nu_5 : \nu_6 \to \nu_1$	150K, 2.10	0.48	150-600	[14]
	ZPLI: $\nu_5 \to \nu_2$	324K, 1.13	0.97	150-350	[13]
	ZPLI: $\nu_5 \to \nu_4$	185K, 0.78	0.66	100-350	[13]
NBW: Yb^{3+}	FIR: $\begin{cases}\nu_6 \to \nu_2\\ \nu_7 \to \nu_4\end{cases} : \nu_5 \to \nu_2$	300 K, 0.26	0.10	300–1000	-
	ACR: $\begin{cases}\nu_2 \to \nu_5\\ \nu_3 \to \nu_6\end{cases} : \begin{cases}\nu_1 \to \nu_6\\ \nu_2 \to \nu_7\end{cases}$	300 K, 0.58	0.17	300–1000	-
	ZPLI: $\nu_5 \to \nu_3$	100 K, 1.92	1.66	30–400	[13]
	ZPLI: $\nu_5 \to \nu_2$	150 K, 0.88	0.84	50–150	[13]
ZBLANP:Nd^{3+}	FIR: $^4F_{3/2}$, $^4F_{5/2} \to {}^4I_{9/2}$	293 K, 1.15	-	296–473	[11]
Silica:Sm^{3+}	FIR: $^4F_{3/2}$, $^4G_{5/2} \to {}^6H_{5/2}$	296 K, 1.84	-	295–473	[26]
YAG:Nd^{3+}	FIR: $^4F_{3/2}$, $^4F_{5/2} \to {}^4I_{9/2}$	293 K, 1.43	-	299–523	[11]
Telluride:Pr^{3+}	FIR: $^3P_1$, $^3P_0 \to {}^3H_5$	293 K, 1.02	-	273–453	[3]
BiLiBaPb: Er^{3+}	FIR: $^4S_{3/2}$, $^2H_{11/2} \to {}^4I_{15/2}$	296 K, 0.44	-	296–603	[25]

References

[1] K. V.Rai, Appl. Phys. B **88** (2007) 297.
[2] K. V.Rai, Appl. Phys. B **87** (2007)323.
[3] K. V.Rai, D. K.Rai, S.B.Rai, Sensor Actuator A, **128** (2006)14.
[4] A.Pandey, V. K.Rai, Rare earth doped materials for temperature sensors. Spectroscopic Techniques for Security Forensic and Environmental Applications ed. Y.Dwivedi, S. B.Rai, J. P.Singh (Nova Publisher USA, 2014) 279–292.
[5] A. S.Camargo, J. F.Possatto, L. A.Nunes, et al., Solid State Communications, **137** (2006) 1.
[6] L. Feng, B.Lai, J.Wang, G.Dua, Q.Su, J. Luminescence, **130** (2010) 2418.
[7] C.Li, B.Dong, Sh.Li, Ch.Song, Chemical Physics Letters, **443** (2007) 426.
[8] G.Liu, L.Fu,Zh.Gao,X.Yang, Z.Fu, Zh.Wang, Y.Yang, RSC Adv. 5 (2015) 51820.
[9] J. L.Kenndey, N.Djeu, Sensors Actuators A, **100** (2002) 187.
[10] N.Rakov, G.Maciel, Applied Physics, **17**, 10, (2017)1223.
[11] S. A.Wade, S. F.Collins, G. W.Baxter, Applied Physics, **94**, (2003) 4743.
[12] H.G.Demirkhanyan, G.G.Demirkhanyan, R.B.Kostanyan,*LaserPhysics* **28.2**,(2018) 025701
[13] H.G.Demirkhanyan, G.G.Demirkhanyan, E.P.Kokanyan, R.B.Kostanyan, M.Aillerie, SPIE Proceedings Series, **8414**, (2012) 8414Q1-7.
[14] H.G.Demirkhanyan, J. Contemp. Physics, **46** (2011) 425.
[15] W. F.Krupke, IEEE J. Sel. Top Quantum Electron, **6** (2000) 1287.
[16] L.D.DeLoach, S.A.Payne,L.L. Chase, L.K.Smith,W.L.Kway, W.F.Krupke, IEEE, J. Quantum Electroics, **29** (1993) 1179.
[17] G. G.Demirkhanyan, Laser Physics, **16,** 7 (2006) 1054.
[18] J.Kawanaka, S.Tokida, H.Nishioka, et. al., Laser Physics, **15** (2005)1306.
[19] G.G.Demirkhanyan, R.B.Kostanyan, Laser Physics, **18,** 2 (2008) 104.
[20] H.G.Demirkhanyan, G.G.Demirkhanyan, V.G.Babajanyan, R.B.Kostanyan, E.P.Kokanyan, J. Contemp. Phys. **43** (2008) 13.
[21] G.G.Demirkhanyan, Thesis of Doctor of Science, Institute for Physical Research of NAN RA, Ashtarak, Armenia, (2008)
[22] L.D.Merkle, M.Dubinskii, B.Zandi, J.B.Gruber, D.K.Sardar, E.P.Kokanyan, V.G.Babajanyan, G.G.Demirkhanyan, R.B. Kostanyan., Optical materials, **27**, N2 (2004) 343.
[23] G.G.Demirkhanyan, V.G.Babajanyan, E.P.Kokanyan.,R.B.Kostanyan, J.B.Gruber, D.K.Sardar, Optical materials, **29**, N8 (2007) 1107.
[24] G.G.Demirkhanyan, H.G.Demirkhanyan, E.P.Kokanyan, R.B.Kostanyan, J.B.Gruber, K.L.Nash, D.K. Sardar, J. of Applied Physics, **105**, N 6 (2009) 063106.
[25] G.Tripathi, V.K.Rai,S.B. Rai,Opt.Mater.,**30** (2007) 20.
[26] R.B.Alves, J.Christol, M.Sun,K.A.Wickersheim, Proc. ISA Int. Conf. and Exhibit,Houston. TX, ISSN. 0065-2814, (1983) 925.